Fortschr. Miner.	52	Beiheft 1	103—122	Stuttgart, August 1974

Excursion B 4

Ries meteorite crater, Germany

With 8 figures and 1 table

The following three articles present an introductory description and interpretation of the Ries crater, its impact formations and outcrops which will be visited by the field excursion. The excursion is guided by W. von Engelhardt, E. Preuss and D. Stöffler.

I. The Ries structure and its impact formations

By
W. v. Engelhardt

With 2 figures

The Ries crater, 24 km in diameter, which is 100 km northwest of Munich (Fig. 1) has been the object of many geological investigations, for more than hundred years. Older theories assumed that the structure was produced by volcanic forces, or even by glaciation. The impact theory, tentatively expressed by Werner (1904) and Stutzer (1936), was first confirmed by the detection of coesite in suevite by Shoemaker & Chao (1961). Later geophysical, geological and petrological investigations provided many further contributions to the knowledge of this crater and its formations, formed by an impact 14.8 million years ago. A theoretical approach to describing the Ries impact as a physical process was published by David (1969). Reviews in the older literature about the Ries were given by Löffler (1925), Kranz (1925—1952), Preuss (1964, 1969) and Dehm (1969). Several articles, representing the knowledge up to 1969, are contained in the volume "Das Ries", edited by Preuss & Schmidt-Kaler (1969). A summarizing review was published by Dennis (1971). The following remarks can only deal with the facts of general importance.

Nearly the whole Ries area has been geologically mapped at the 1:25,000 scale (see Preuss 1964, Hüttner, Schmidt-Kaler & Treibs 1969). The mapping was done by several people with different theoretical backgrounds, over a long period of time (since 1925), and before the impact origin of the crater was recognized. Therefore, the maps, although representing extremely careful and reliable observations, do not provide all the information which is desirable from the point of view of the impact theory. A geological map (scale 1:100,000) of the whole Ries area was recently published by Hüttner, Schmidt-Kaler & Treibs (1969). It represents a synopsis of the information available to 1969.

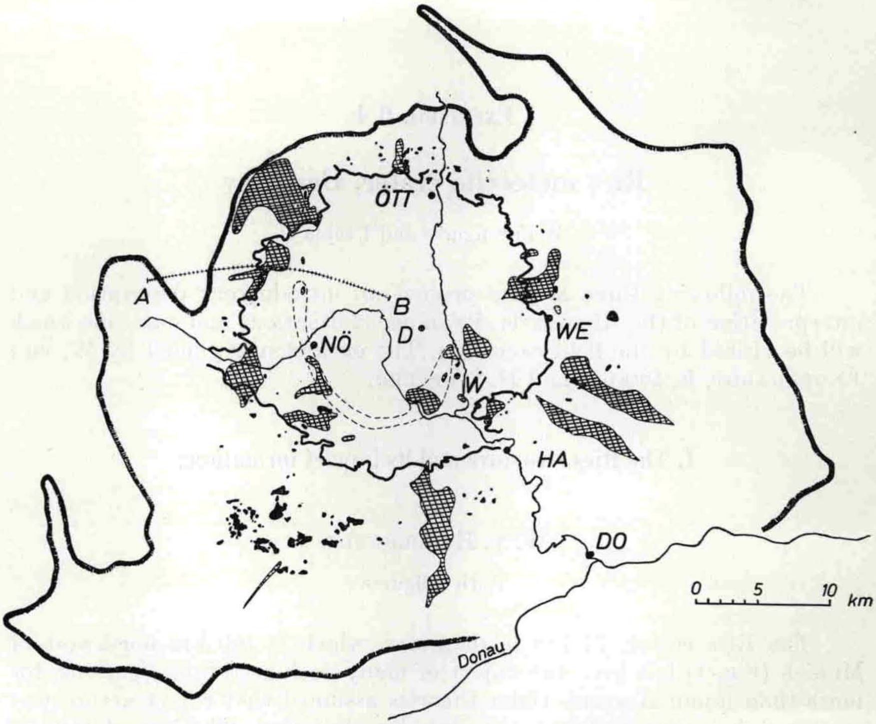

Fig. 1. Ries crater, Germany. D = drill hole of Deiningen W = drill hole of Wörnitzostheim A—B = seismic profile, Fig. 2.
The outermost contour defines the area around the crater covered by multicolored breccia, consisting of fragmental sedimentary rocks. Hatched areas are rich in crystalline rocks excavated from the basement as large uniform blocks or monomict and polymict breccias. Black spots are occurrences of suevite. The morphological crater rim is represented by the 500-m contour line in the southern half and the 460-m contour in the northern half of the structure, respectively. The horseshoe-shaped ring of hills surrounding the central crater is indicated by a dashed line.

In the Ries area the crystalline basement (gneisses, granites, amphibolites of Hercynian age) is overlain by a sequence of Mesozoic sediments, roughly 700 m thick. The sequence consists of about 300 m of Upper Jurassic limestone, about 150 m of Middle and Lower Jurassic sandstones and shales, about 250 m of Upper to Middle Triassic (Keuper) marls, sandstones and shales and Lower Triassic or even Permian sediments of variable thickness. The sediments dip gently to the south. The hard Upper Jurassic limestone forms an escarpment, the Swabian Alb, striking west-southwest. At the time of the impact the escarpment crossed the present Ries plain close to its center.

The flat bottom of the Ries depression has an average elevation of 420 m above sea level. The surrounding hills reach elevations of over 600 m in the south, where they are built up by Upper Jurassic limestone, but only 500 m in the north, where they consist of softer Middle Jurassic, Lower Jurassic and Keuper rocks. The basin rim has a somewhat polygonal outline, probably due to pre-existing fracture systems. The central part of the basin forms a flat plain of circular outline, about 10 km in diameter. It is surrounded by a horseshoe-shaped ring of hills up to 50 m in height which is open to the north. Between this inner ring of hills and the outer rim is a marginal zone of hummocky and irregular relief. The interior of the basin is filled by Tortonian and Sarmatian (Upper Miocene) lake sediments, covered in part by alluvial and Pleistocene deposits. Upper Miocene fresh-water limestones occur on top of the hills of the horseshoe ring and along the inner slope of the outer rim. At a distance of a few km (at most 5 km), the present rim is surrounded by a watershed. Two rivers enter the basin, the Wörnitz from the north and the Eger from the southwest. The Wörnitz river, after joining the Eger, leaves the basin through a narrow outlet in the southeast. Inlets and outlets represent old valleys already existing before the impact.

Johnson & Vand (1967) carried out an harmonic analysis of the Ries crater morphology based on 1:25,000 topographic maps. A main rim was found, 24 km in diameter, and two secondary ones, 34 and 45 km in diameter, respectively. No geological or other field evidence is known for ground movements at such great distances outside the crater. The contours of the rims obtained in this analysis are slightly elliptical. The major axis has a general north-northwest — south-southeast direction. Masses excavated by the impact and raised from the crater floor occur in the horseshoe ring, within the hummocky zone between this ring and the outer rim and as an ejecta apron outside the crater. Impact breccias have also been found in boreholes below the lake sediments in the central crater.

Within and around the Ries crater the following main types of impact formations can be distinguished and mapped:

(1) Blocks of shattered but uniform masses of Mesozoic sediments, sometimes more than 1 km in size. Predominant are blocks and intensely fractured masses of Jurassic limestones. Such masses occur within the marginal zone of the crater and outside the rim, within the region occupied by multicolored breccia. The participation of lower members of the stratigraphic column diminishes with increasing distance from the crater (Hüttner, 1969). Smaller fragments of Upper Jurassic limestone also occur south of the Danube as boulders at the base of Pleistocene deposits (Reutersche Blöcke) and embedded in Upper Miocene fluviatile sediments which have the same age as the Ries event. Most of the known occurences in Miocene sediments are located 50—70 km south and southeast of the Ries center. An isolated mass of heavily fractured limestone, about 2 m in diameter, has been found 140 km southeast of the crater (Hüttner, 1969; Herold, 1969; Engelhardt, unpublished observations).

(2) Multicolored breccia (Bunte Breccie) is a weakly shocked polymict breccia composed of all kinds of sedimentary rocks in variable proportions, with a small admixture of material from the crystalline basement. The components range in size from large blocks to the finest grains. Multicolored breccia occurs within the marginal zone of the crater and outside of it. Around the crater the multicolored forms an apron extending from the rim

up to 26 km to the southwest and up to 24 km to the south-southeast, but only 3—4 km to the north. In the south the extension of the breccia is interrupted by the Danube valley. The thickness is very variable; the average may be 20—24 m, but maximum values up to 80 m have been observed in the southeast. The amount of older sediments and of crystalline material in the breccia diminishes with increasing distance from the center. Indications of shock metamorphism in the multicolored breccia are a few quartz grains with planar deformation structures and some fragments of crystalline rocks in stages I and II of shock metamorphism. The multicolored breccia was moved along the ground, as can be concluded from striations on the surface of underlying limestone, pointing to the crater centre, and from strong interaction and mixing with local unconsolidated Miocene sediments in the south (HÜTTNER, 1969; SCHNEIDER in ENGELHARDT et al., 1969, 1971).

(3) Fragmental material from the crystalline basement occurs as uniform blocks of granite or gneiss, up to some 100 m in size, or as monomict and polymict weakly to moderately shocked breccias. The larger blocks are situated predominantly within the horseshoe ring. Crystalline breccias occur at the inner ring, within the marginal zone and outside the crater, predominantly in two rays extending to the south and southeast. Monomict breccias consist of fragments of one crystalline rock and show only minor shock effects (up to stage I of shock metamorphism). Polymict breccias are mixtures of different gneisses, granites and amphibolites. Shock effects include stages I and II of shock metamorphism, but no melting. Coesite and stishovite have been found in these breccias (HÜTTNER, 1969; DRESSLER, GRAUP & MATZKE, 1969; ABADIAN, 1972; GRAUP, 1971; STÖFFLER in ENGELHARDT et al., 1969).

(4) Suevite is a strongly shocked breccia consisting of crystalline rock fragments, a few sedimentary rocks, mineral fragments (predominantly quartz), glass fragments and glass bombs in a groundmass of montmorillonite. Crystalline rock and mineral fragments occur in all stages of shock metamorphism up to complete melting. Coesite and stishovite have been found in shocked rock fragments (STÖFFLER, 1971b). Characteristic constituents are aerodynamically shaped bombs (Fladen) consisting of a heterogeneous schlieren-rich, mostly devitrified glass with inclusions of many mineral fragments (predominantly quartz), lechatellerite and vesicles. The chemical composition of the glass of all suevite occurrences is very uniform, corresponding to a gneiss of granitic norm (HÖRZ, 1965; ENGELHARDT & HÖRZ, 1965; ENGELHARDT, 1967). The Ni-content seems to be higher than that of the crystalline source rocks (STAEHLE, 1970). As can be concluded from the remanent magnetization, the average temperature of the suevite at the time of its deposition was above the Curie temperature of magnetite, i.e. >580 °C. Vertical vents formed by escaping vapor or gases and early hydrothermal alterations show that the suevite mass included a certain amount of volatiles.

Suevite occurs (1) as a blanket underlying the lake sediments in the central basin (fall-back breccia) and (2) at the surface as isolated spots in the marginal zone and outside the crater, especially to the south and east (fallout breccia), up to 20 km from the crater rim. In most cases fallout suevite is underlain by multicolored breccia. The occurrences at the surface may be remnants of an originally more continuous blanket of variable thickness. The present spot-like occurrences may represent thicker suevite accumulations trapped in local pockets of the hummocky multicolored breccia relief. Suevite was deposited as the last of all masses ejected from the crater. As can be concluded from structures at the lower contact (SCHNEIDER, 1971), the suevite mass, as a hot density current, overflowed the crater rim and rolled over the first-formed deposits of multicolored breccia. Because the shapes of the bombs indicate their rapid flight through the air it is probable that the suevite current developed from the breakdown of an eruption column ejected more or less vertically from the crater center. Suevite breccias below the lake sediments represent that part of the material which landed within the crater. Although suevite deposits outside the crater never show laminated or dune-like structures their mode of formation may be somewhat similar to that of volcanic base surge deposits as described by WATERS & FISHER (1971). (HÜTTNER, 1969; ENGELHARDT et al., 1969, HÖRZ 1965; STÖFFLER 1966; FÖRSTNER 1967; CHAO 1968 and in unpublished records).

(5) Impact melt. Red vesicular rocks, occurring in two small outcrops near the eastern rim (Polsingen, Amerbach), may represent impact melts. The rocks show a fluidal texture and contain many crystalline fragments in a groundmass consisting of feldspar laths, pyroxene, some cristobalite and hematite. They may be outlying tongues of impact melt rock sheets which occur deeper in the crater (ENGELHARDT et al., 1969; DENCE, 1971).

Shatter cones are very rare in the Ries. Some not very well developed cones in a brecciated limestone from a crystalline breccia and some small ones in crystalline fragments have been found near the eastern rim. A large granite block with many well-developed shatter cones has been found in multicolored breccia at the southeastern rim (DRESSLER, GRAUP & MATZKE, 1969; GRAUP, 1970, unpublished observations; ENGELHARDT, 1970, unpublished observations).

Results of gravity measurements carried out in the Ries area have been summarized by JUNG, SCHAAF & KAHLE (1969) and KAHLE (1969). The residual field obtained by subtraction of the regional field from the measured gravity values shows a centrosymmetrical negative anomaly the center of which (—18 milligal) is located at the topographical Ries center. By integrating the gravity anomaly, a total deficient mass is obtained between 6.8×10^{16} and 7.7×10^{16} g.

The Ries crater shows negative magnetic anomalies which are mainly located within the inner crater. The measurement of the magnetization of suevite has shown that the anomaly is due to a suevite layer of varying thickness, up to 400 m, in the central crater (POHL & ANGENHEISTER, 1969).

Refractive seismic experiments from 1948 to 1952 and recent reflection profiles have revealed the complicated structure of the Ries crater. A profile, based on reflection data from outside the crater through the western rim and ending in the center (18 km), is shown in Fig. 2. An inner crater, 10 km in diameter, is surrounded by the inner horseshoe rim. Within the inner crater Tertiary sediments of about 350 m maximum thickness have been deposited after the Ries event. Below these sediments lies a layer of suevite of varying thickness, up to 300—400 m. The layer underlying the suevite is a breccia of unknown composition. The inner ring is probably composed of fractured crystalline rocks. The marginal zone between the ring and the outer rim is mostly filled with various breccias. The western rim is clearly indicated by the abrupt disappearance of the reflections in the undisturbed Mesozoic layers and from the surface of the basement (ANGENHEISTER & POHL, 1969).

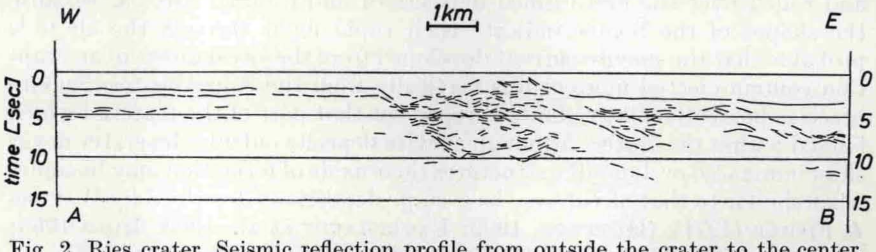

Fig. 2. Ries crater. Seismic reflection profile from outside the crater to the center. For location of the profile, see Fig. 1 (ANGENHEISTER & POHL, 1969).

Two drill holes have penetrated the lake sediments. The hole at Deiningen, approximately 1 km south of the topographic center, has revealed suevite underlying a sequence of 310 m of lake sediments. The hole at Wörnitzostheim, located in the southeast of the basin, in the marginal zone, close to the inner ring, has revealed 20 m of lake sediments, underlain by 80 m of suevite. Below the suevite lies 1.3 m of granite and multicolored breccia composed of Keuper and Middle Jurassic, in an inverted sequence (FÖRSTNER, 1967)[1].

The distribution of ejecta masses is not centrosymmetrical around the Ries crater. Multicolored breccia, crystalline breccias and suevite occupy larger areas south and southeast of the crater than to the north and northwest. To some degree, the present distribution may be influenced by erosion which was more intense in the north than to the south. However, the present asymmetry can probably not entirely be attributed to erosion alone. It might be that more brecciated material was ejected and deposited to the southeast and south than to the north and northeast. Asymmetrical features can also be recognized in the morphology of the crater. The horseshoe ring of crystalline material raised to the surface is open to the north or northwest and JOHNSON & VAND (1967) showed that the topographic crater shows an elliptical contour, the long axis pointing to the southeast. It is probable that these asymmetries originate from an oblique incidence of the impacting body which came in at a low angle from the north-northwest.

Age determinations (K—Ar) of glassy bombs from several suevite occurrences gave 14.8 ± 0.7 m.y. These values have been confirmed by fission track measurements. The same age was found for the moldavites and bentonitic glass tuffs which occur near Landshut, Bavaria, 90 km southeast of the Ries center, in Upper Miocene sediments. It was suggested that both moldavites and glass tuffs were produced by the Ries impact. Several theories have

[1] Note added in proof: A third drill hole, "Nördlingen 1973", located 4 km north of Nördlingen, has been completed in January 1974. The hole reached a depth of 1206 m and penetrated the following profile: 0—325 m: lake sediments, 325—605 m: suevite, 605—1206 m: crystalline breccia (Geol. Bavarica **72**).

been proposed about source material and mode of transportation, such as melting of surface material and ejection of jets early in the impact process, or on condensation from a silicate vapor. The chemical composition of moldatives and Bavarian glass tuffs is markedly different from that of Ries glass bombs (COHEN, 1961, 1963; GENTNER, LIPPOLT & SCHAEFFER, 1963; GENTNER & WAGNER, 1969; DAVID, 1969; ENGELHARDT & HÖRZ, 1965; ENGELHARDT, 1967).

II. Cratering mechanics, impact metamorphism and distribution of ejected masses of the Ries structure — An introduction

By

D. STÖFFLER

With 6 figures and 1 table

The following introduction is partly based on the general information about the Ries crater and its impact formations given by W. VON ENGELHARDT in the first part of this paper. It is the aim of this section to present a brief review of some aspects of cratering mechanics, impact metamorphism, and ejecta distribution with respect to the conditions of the Ries event. This review cannot give a complete coverage of all aspects of the formation of the Ries crater. For more detailed information the reader is referred to the special literature.

Impact and excavation mechanics

Although mineralogical, petrographical, geophysical and geological data obtained mainly in the past decade (see collection of papers in PREUSS & SCHMIDT-KALER, 1969) have strongly and consistently proved the impact origin of the Ries crater, the exact physical impact conditions, that is the velocity, size, and nature of the cosmic body as well as its orbital parameters are not known. However celestial mechanics tells us that the impact velocities of meteorite bodies with respect to the Earth range from about 11 to 70 km/sec. Velocities in the 15—40 km/sec range have the highest probability (MILLMAN & MCKINLEY, 1963). Moreover we know from cratering experiments that the kinetic energy of the projectile is proportional to the size of the produced crater and that within certain limits the morphological parameters of a crater do not depend on the angle of impact at constant kinetic energy except for very oblique angles (GAULT et al., 1968; GAULT, 1973). These relations are exactly valid only for small-scale impact craters with energies up to some 10^{16} erg (GAULT, 1973). Extrapolation of the experimental data and additional information from large-scale high-explosive and nuclear explosion craters (Cratering Symposium, 1961) result in a most probable value of the total energy of the Ries event of $E = 10^{26}$ to 10^{27} erg. Previous estimates of this energy are somewhat higher (Preuss, 1964; DAVID, 1969). For a given impact velocity v the mass of the projectile m can be calculated according to $E = \frac{mv^2}{2}$. If this mass is then converted to the dimensions of a stony and iron meteorite sphere for an impact velocity of 20 km/sec, the diameter of this sphere would be 230 m and 317 m, respectively in the case of $E = 10^{26}$ erg, or 495 m and 683 m, respectively in the case of $E = 10^{27}$ erg.

The physical process of cratering by a meteorite impact with the conditions mentioned above can be briefly described as follows. For any detailed explanation the reader is referred to special papers (GAULT et al., 1968; DAVID, 1969; ENGELHARDT, 1974). Upon impact the target rocks and the projectile are compressed with approximately one half of the impact velocity (if it is a stony meteorite) through the propagation of two shock waves which proceed hemispherically into the target and the projectile with roughly 4/5 of the impact velocity (Fig. 3). From the known Hugoniot equation-of-state data for rock and meteorite material the peak pressure and temperature at the point of impact can be calculated approximately: about 4.5 megabar (ca. 4.5×10^6 atm) and 15000° for a stony meteorite with a density of 3.0 g/cm³ and an impact velocity of 20 km/sec (DAVID, 1969). For a short period of time which is less than 0.03 sec, until the shock wave reaches the rear side of the projectile, the projectile and part of the target rocks are kept under these extreme conditions. They cause immediate vaporization of the affected material. At this point the main process of excavation starts by the propagation of rarefaction waves which run into the target from any point where the proceeding shock wave reaches the free surface. The rarefaction wave accelerates the target material in an upward direction. By the interaction of this motion with the particle motion behind

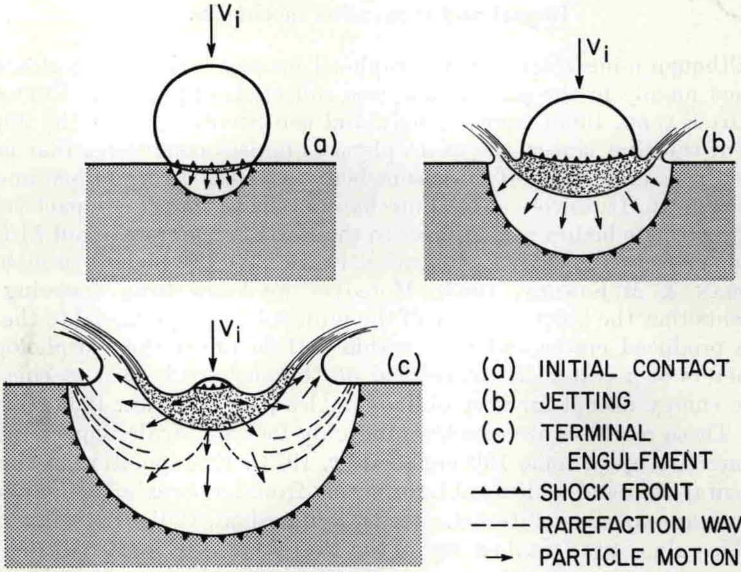

Fig. 3. Schematic representation of the shock wave propagation and particle motion at various stages of the vertical impact of a spherical body on a plane solid surface (modified after GAULT et al., 1968).

the shock wave which is more or less horizontal at the target surface, the affected material is ejected into divergent, oblique ballistic trajectories. The ejection velocity decreases strongly as the shock wave proceeds into the target. Thereby the crater grows as long as the energy of the shock wave is sufficient to accelerate the surface material. At this point where the crater rim is formed, the target rocks are broken into large blocks which are only slightly displaced or tangentially shifted. The continuous ejection of rocks during crater growth produces a continuous ejecta blanket in which the pre-impact stratigraphy is inversed and the proportion of rocks from deeper levels of the crater decreases with radial distance. The strongly shock compressed central and deepest part of the target near to the vaporized projectile is affected by a more vertical or even convergent upward motion due to the expansion of the compressed material. This motion is directed radially toward the center of the crater. Obviously the interaction of this motion of liquid and solid rock material with the expanding rock vapor leads to the ejection of a "suspended load" of molten, highly shocked, and shock comminuted material which forms the suevite breccia. It is deposited as a discontinuous, hot thin layer on top of the continuous bulk ejecta blanket called Bunte Breccia. A short period of time elapses between the deposition of both types of ejecta units. The different excavation mechanics for both units explain their marked compositional and shock metamorphic differences and the sharp discontinuity between them (Engelhardt et al., 1969; Hüttner, 1969; Schneider, 1971).

Progressive shock metamorphism of rocks

As discussed above the peak pressure and temperature of the propagating shock wave are steeply decreasing with radial distance from the point of impact. This pressure attenuation is mainly caused by the hemispherical geometry of the shock wave propagation which transfers the internal energy of the compressed matter into a steadily increasing volume of rock material. The radial decrease of pressure is approximately proportional $r^{-3/2}$ (r = radial distance from the point of impact; Gault & Heitowit, 1963). According to this pressure decay hemispherical zones of constant pressure and temperature decreasing with radial distance exist during the passage of the shock wave. The shock zoning is shown schematically in Fig. 4 for the dimensions of the Ries event. Within these zones of progressive shock metamorphism which predominantly affect the crystalline basement rocks, the most abundant rock-forming minerals such as quartz, feldspar, hornblende, pyroxene and biotite undergo very characteristic shock effects which are irreversible upon pressure release. Based on laboratory shock experiments with these minerals and their parent rocks it was possible to correlate the various "post-shock" effects with a pressure-temperature scale so that the observed deformation and transformation phenomena can now be used as natural pressure and temperature indicators (Fig. 5, for details see review in Stöffler, 1972, 1974). Quartz and feldspar show the greatest variety of different shock effects in the 100 to 500 kbar range and hence are most useful as petrographic pressure indicators.

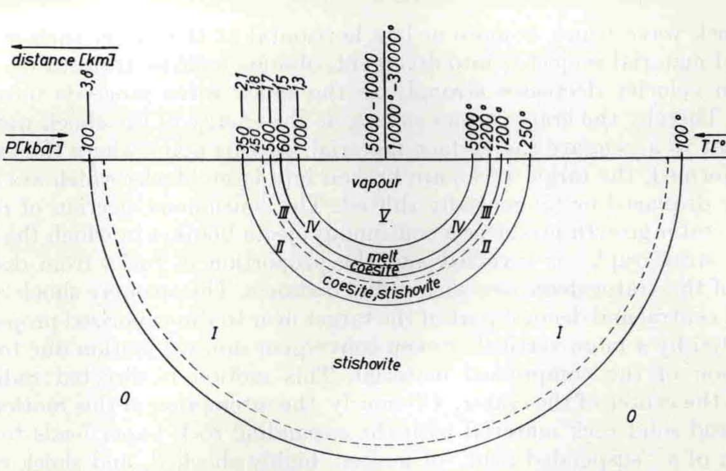

Fig. 4. Progressive zones of shock metamorphism as classified by Stöffler (1971 a). The shock zones present in the bedrocks of an impact crater during the passage of the shock wave may deviate from the hemispherical model, which is schematically adapted to the dimensional parameters of the Ries event as given by David (1969). From Stöffler (1971 b).

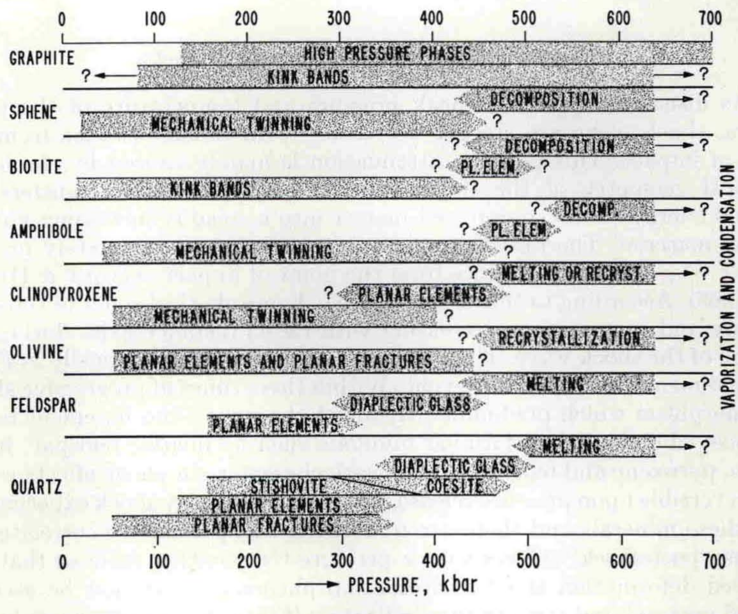

Fig. 5. Schematic representation of the pressure ranges in which various types of residual shock effects are produced in the most frequent rock-forming minerals. Question marks indicate uncertain pressure limits. The diagram is based on experimental data and natural observations referenced in Stöffler (1972).

Table 1. Stages of progressive shock metamorphism of crystalline rocks from the Ries crater according to STÖFFLER (1971a).

Stage	peak pressure in kbar	postshock temperature in °C	Post-shock effects in quartz, feldspar or total rock	Textural properties of the rock fragments in the breccias
I	≃ 100	≃ 100	Diaplectic crystals with planar deformation structures (isotropic lamellae) parallel to crystallographic planes and with lowered density, refractive index and birefringence. Stishovite within quartz	Primary texture of the rock is preserved. Intense fracturing
II	≃ 350	≃ 300	Diaplectic glasses as pseudomorphs of quartz and feldspar grains. Coesite and stishovite within diaplectic quartz glass	Primary texture preserved, but clouded appearance of the framework silicates
III	≃ 450	≃ 900	Normal feldspar glass with vesicles and flow structures. Diaplectic quartz glass, coesite (and sometimes traces of stishovite) within diaplectic quartz glass	Primary texture partially destroyed by selective melting. Porous or pumice-like texture
IV	≃ 550 —600	≃ 1300 —1500	Total melting of all mineral phases and mixing of the melts. Remnants of isolated quartz and feldspar glasses with vesicles and flow structures	Primary texture totally destroyed, aerodynamically-shaped glassy bombs
V	> 800	> 3000	Silicate vapor	

The existence of zones or stages of progressive shock metamorphism in the crystalline basement rocks of the Ries crater was first discovered in the crystalline inclusions incorporated in the suevite breccia. Suevite was found to contain a chaotic mixture of rock fragments of different degrees of shock which had been ejected from different depths of the basement (STÖFFLER, 1965, 1966; CHAO, 1968). On the basis of the observed shock effects in quartz and feldspar these rocks could be classified into 5 main stages of shock metamorphism which are described in Table 1. CHAO (1968) proposed a somewhat different classification for the granitic rock suite of the Ries crater. The concept of classification given in Table 1 which is applicable to all dense, crystalline rocks (STÖFFLER, 1971) is important for the interpretation of the origin and excavation mechanics of the various types of impact formations which have been found in the Ries area (see VON ENGELHARDT in Part I).

Characteristics of the distribution of the Ries ejecta formations

As discussed by W. von Engelhardt in the first part of this paper the impact formations of the Ries crater can be classified into two main types:

a) *Bunte Breccia* in the widest sense represents the majority (probably more than 95%) of the ejecta blanked mass of the crater. Bunte Breccia comprises different subgroups such as the large, monomict shattered blocks or masses of sedimentary or crystalline rocks, the polymict crystalline breccias, and the more fine-grained Bunte Breccia sensu stricto into which the former two groups may be incorporated.

b) *Suevite* and *impact melt rocks*. Suevite consists predominantly of fragments of crystalline rocks of all possible stages of shock metamorphism. 20—75% of these inclusions are shock melted rocks. Suevite and the rare coherent masses of recrystallized melt rocks exposed near Polsingen and Amerbach represent the highly shocked central part of the crater. This is only a small percentage of the total displaced mass.

Both types of impact formations occur in the ejecta blanket ouside the crater and in the fallback material inside the crater as well though their composition is different in both locations. The presence of a suevite blanket on top of the fallback material is known from the drilling cores of Deiningen (depth: 350 m) and of Nördlingen (depth: 1206 m). This suevite has a fragmental matrix without glass; only a few of the abundant coarser inclusions are shock melted rocks. The throwout suevite, however, is characterized by a glass-rich fragmental matrix and a high abundance of molten rock inclusions which form typical glassy bombs.

The Bunte Breccia inside the crater below the suevite blanket is a crystalline rock breccia which is almost free of Jurassic and Triassic sedimentary rocks. Its counterpart in the throwout ejecta blanket consists mainly of large blocks and smaller fragments of sedimentary rocks with a small admixture of crystalline rocks which may be shocked up to stage II (Table 1). In a zone between the inner ring of uplifted crystalline rocks and the present morphological rim (compare Engelhardt in part I) the ejecta material is extremely blocky. The "megablocks" are mainly derived from the sedimentary strata. They are mixed together with a few blocks of crystalline rocks with finer grained Bunte Breccia which also contains pockets or dikes of polymict breccias (Abadian, 1972). Probably this zone represents the primary rim area which upon excavation of the crater was structurally deformed by slumping and faulting because of the isostatic readjustment of the crater. Thereby secondary uplifting of the inner ring of crystalline rocks may occur which enhances a possible primary uplifting produced during cratering as a result of a change of the particle motion at the density discontinuity between sedimentary and crystalline basement rocks.

The continuous ejecta blanket outside the crater may be characterized by a typical horizontal and vertical variation of some compositional and structural properties (Fig. 6).

From the present surface geology of the ejecta blanket it is inferred that only the Upper Jurassic rocks are represented throughout the whole blanket.

Generally, in a horizontal section of the ejecta blanket we find that the deeper the original location of a rock unit was before impact the nearer to the crater rim it is deposited upon excavation (Figs. 7 and 8). The number and size of blocks, in particular those of the Upper Jurassic limestones decrease with increasing radial distance from the center (HÜTTNER, 1969; GALL,

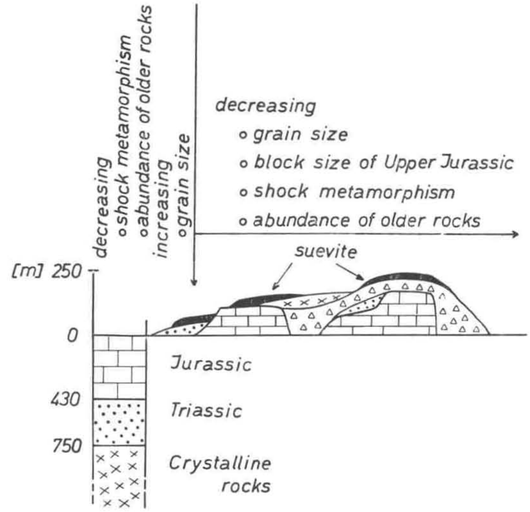

Fig. 6. Variation of stratigraphic relations within the Ries ejecta blanket with respect to the pre-impact stratigraphy of the Ries target.

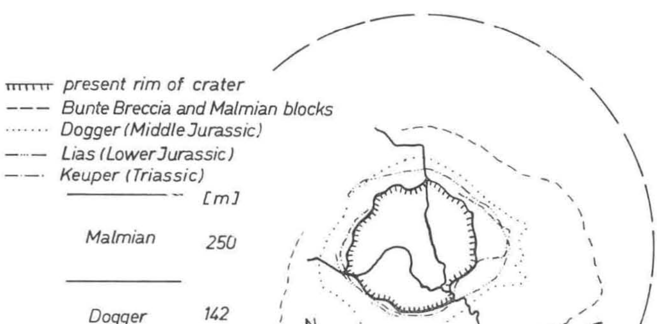

Fig. 7. Radial distribution of rocks from different stratigraphic levels within the ejecta blanket of the Ries crater. The pre-impact stratigraphy is given in the left part of the graph. The outer circle indicates the presumable extension of the primary continuous ejecta blanket.

1974). In general, the grain size of the Bunte Breccia decreases in the same way (SCHNEIDER, 1971). A relative increase of the number of mappable blocks from the uppermost Malmian (δ—ξ) over blocks from the lower Malmian (older than δ) with increasing radial distance was observed by SCHRÖDER & DEHM (1950) and HÜTTNER (1969) and was quantitatively measured by GALL et al. (1974). In an outer zone of the ejecta blanket an increasing amount of locally derived pre-Riesian surface material, mostly Tertiary sand, is incorporated into the Bunte Breccia (HÜTTNER, 1969; SCHNEIDER, 1971; GALL, 1974). This is probably due to the fact that the ejecta thrown to the farthest distance have the highest ejection and landing velocity. The mechanism of secondary mass transportation by landing ejecta is very commonly observed at lunar craters (OBERBECK et al., 1974).

Vertical sections of the Ries ejecta blanket show a typical inversed stratigraphy with respect to the pre-impact setting of rocks. This stratigra-

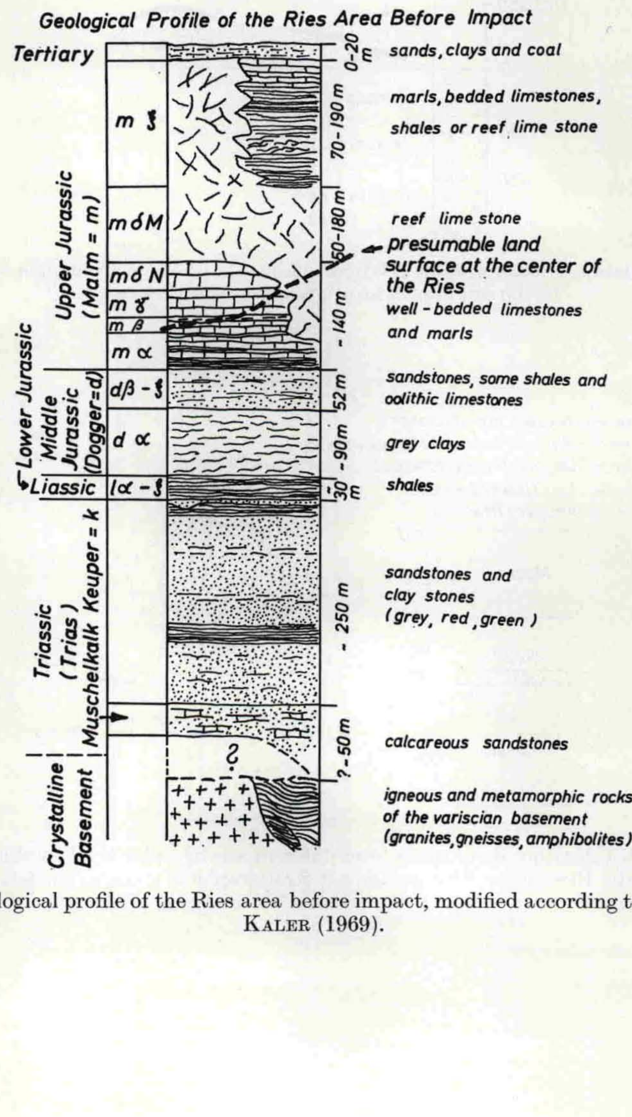

Fig. 8. Geological profile of the Ries area before impact, modified according to SCHMIDT-KALER (1969).

phy is discontinuous and locally incomplete (Figs. 6 and 8). An increase of particles from lower stratigraphic levels of the pre-impact section was found in the polymict, finer grained Bunte Breccia going from bottom to top (SCHNEIDER, 1971). He also observed an increase of the number of shocked particles in the same direction.

The thickness of the ejecta blanket is locally very variable according to the pre-impact relief of the ground zero surface. The average thickness of Bunte Breccia ranges from 80 m near the rim (HÜTTNER, 1969) to some few meters in a radial distance of 35 km (GALL, 1974; GALL et al., 1974). Locally up to 140 m of Bunte Breccia was found in a radial distance of 22 km from the center of crater (BIRZER, 1969). Textural, stratigraphic and grain size properties of the few distant occurrences of Bunte Breccia north of the crater where the post-Riesian erosion is most pronounced indicate that the primary distribution of Bunte Breccia must have been more or less centrosymmetrical with respect to the crater up to a radial distance of more than 40 km (GALL et al., 1974). On the basis of an average thickness of Bunte Breccia of 20 to 25 m, as indicated by the field geology (GALL et al., 1974) we have to expect a volume of 110 to 138 km^3 deposited between the radii of 11 km (primary rim area) and 42 km. According to the currently used excavation models and to the reconstructed primary cross section of the crater the displaced volume which contributed to the ejecta blanket beyond the rim, should be in the order of 190 km^3 (STÖFFLER et al., 1974). About 5—8 km^3 of this volume accounts for the high velocity ejecta (vapor and melt) part of which may have been deposited beyond the vicinity of the continuous ejecta blanket.

III. Description of outcrops and quarries in the Ries area

By
W. v. ENGELHARDT and D. STÖFFLER

1. Holheim, Siegling quarry. Quarry in operation at the southwestern rim near Holheim, 4 km SW of Nördlingen. In the lower part of the quarry highly shattered and brecciated Upper Jurassic limestone is exposed, which probably belongs to an allochthonous huge block. This block is covered by Bunte Breccia, mainly gray shales of the Middle Jurassic (Dogger α). The surface of the limestones has been polished and scratched by the movement of the Bunte Breccia. The direction of the movement as to be seen from the grooves was radially outward from the center of the Ries.

2. Harburg, Märker quarry. Quarry in Upper Jurassic limestone (cement factory Märker) S of Harburg, at the western slope of the Wörnitz valley, 3 km SE of the rim. The Wörnitz valley, cut into Upper Jurassic limestone, was filled by Bunte Breccia masses ejected from the Ries crater. The main part of these deposits were later eroded by the river draining the Ries basin. Within the quarry Upper Jurassic limestone and Bunte Breccia lining the valley slopes and bottom are exposed. At this place the Bunte Breccia consists of large masses of the various sedimentary rocks (mainly Upper Jurassic limestone, Middle Jurassic clay, Keuper sandstone) embedded in a fine grained matrix breccia containing also some rock fragments from the crystalline basement.

3. Ronheim, Bschor quarry. The quarry, situated at the southeastern rim near Harburg, is operated within shattered autochthonous Upper Jurassic limestone (Malm Delta-Dickbänke). The top of the limestone has been polished and scratched by Bunte Breccia which now overlays the limestone surface. The striations within this surface are directed toward the center of the Ries basin. The Bunte Breccia, approximately 5 to 10 m thick, consists of fragments of crystalline rocks, shales and sandstones of the Upper Triassic (Keuper), sandstones of the Middle Jurassic (Dogger), limestones of the Upper Jurassic (Malm) and sands of the Tertiary. The grain size of the fragments is broadly variable. Blocks of granitic rocks up to several meters in diameter have been observed. The crystalline inclusions have been shocked up to stage II. No real shock effects have been observed in the sandstone fragments. A shatter-coned granite fragment has been found recently.

4. Nördlingen, Leopold-Meyers-Keller. Exposure of a polymict crystalline breccia in the southern outskirts of the city of Nördlingen (Galgenberg). The crystalline breccia is underlain by Bunte Breccia and covered by Upper Miocene fresh water limestone. The breccia consists of fragments of various basement rocks: 16% granites, 33% gneisses of dioritic to granodioritic composition and 51% amphibolites. 3% of the fragments show no indication of shock, 48% belong to shock stage I and 49% to shock stage II (Abadian, 1972).

5. Gundelsheim, Teich quarry. Autochthonous Upper Jurassic limestone (Malm Delta — Dickbänke) with a polished surface and Bunte Breccia on top of it are exposed within this quarry which is about 8 km ENE of the crater rim. The striations of the limestone surface again point toward the center of the Ries. Bunte Breccia, up to 7 m thick, consists of a matrix of yellow-brown to gray clays of the Tertiary, in which fragments of Upper Jurassic limestone and Tertiary shales up to several meters in diameter are embedded. Fragments of crystalline rocks and Triassic sediments are very rare. Some Jurassic limestone fragments are well-rounded. The crystalline rock inclusions belong to shock stages 0—II. Note the increasing amount of pre-Ries surface rocks incorporated into the Bunte Breccia as the distance from the crater rim increases (Schneider, 1971).

6. Otting, Märker quarry. Suevite quarry in operation, NW of the village Otting, 5 km E of Wemding and the rim. The contact between the underlying Bunte Breccia and the suevite is exposed in the southern part of the quarry. The boundary dips to the N. In the northern part of the quarry the thickness of suevite amounts to about 25 m. A chilled zone at the base of the suevite, about 1 m thick, is exposed in the southern part of the quarry. In the northern part the upper chilled zone, some meters thick, is preserved. Both chilled zones are characterized by glassy bombs which are not devitrified.

Vertical vents produced by escaping gases and vapors occur in various places. Secondary montmorillonitization (yellow colors) can be observed at the contact to the Bunte Breccia and withing an area of the northwestern wall of the quarry. Fresh samples of suevite, glass bombs and crystalline rock inclusions in all stages of shock metamorphism can be best collected in this outcrop.

7. Polsingen. Small old quarry in "red suevite", S of the village of Polsingen near the crater rim, 5 km north of Wemding. The socalled "red suevite" of Polsingen is unique in composition and texture. It consists of a reddish, vesiculated matrix of devitrified glass which includes a large number of mineral fragments and fragmental crystalline rocks, up to about 30 cm in size. These show various stages of shock metamorphism but all are strongly recrystallized in contrast to the inclusions in the normal suevite. Coesite is still present in some of the inclusions. Fragments of sedimentary inclusions have not been observed. The whole mass is similar to a pseudovolcanic impact melt as known from deeply eroded Canadian and Scandinavian impact sites. Except at Amerbach, 3 km S of Polsingen, no other occurrence of this kind of rock is known.

8. Hainsfahrt, Aumühle qarry. Old suevite quarry, 2.5 km NNE of Öttingen, 1.5 km NE of the rim. Suevite overlies Bunte Breccia, which shows a hummocky relief. The chilled zone at the base of the suevite, containing non-devitrified glass bombs is about 1 m thick. In the north-eastern part of the quarry the suevite has a more yellow color and contains fewer and smaller rock fragments and glass bombs.

9. Maihingen, Klostermühle—Langenmühle. Outcrops of crystalline shattered masses and of a polymict crystalline breccia, near the northwestern rim, about 10 km north of Nördlingen. The main volume of this crystalline area consists of a huge block of gneiss with biotite, hornblende, and garnet which is not brecciated but highly fractured showing no typical shock effects. It must have been uplifted as a whole at least 500 m from the pre-Ries crystalline basement. A dike of polymict crystalline breccia up to 1 m thick cuts through the gneiss mass subvertically. Fragments consist of biotite gneiss (58%), granite (18%), amphibolite (18%) and hornblende-gneiss (6%) with variable degree of shock (stage 0: 27%, stage I: 10%, stage II: 61%, stage III: 2% (?)) (Abadian, 1972). These rocks are strongly affected by montmorillonitization and hence are friable in contrast to the country rock.

10. Lehberg. New quarry in a large block of crystalline rocks near the western rim, 2 km SW Marktoffingen. The whole unit consists of biotite gneiss and garnet-cordierite-gneiss with some amphibolite which are in contact with a biotite granite. All rocks are weakly shocked (stage 0 and, rarely, stage I), but heavily shattered. Most conspicuous is a set of parallel thrust planes which are oriented about 108°/20—30 °N. Some polymict Bunte Breccia occurs on top of the crystalline unit, and as thin intrusive-like dikes cutting through it in a similar way as it is observed in the lower part of the drilling core of Nördlingen.

11. Zipplingen. In a road cut north of Zipplingen suevite breccia is exposed which forms an exceptionally hard rock. Fragments of crystalline rocks are very abundant. Gneisses of dioritic and quartzdioritic composition and amphibolites prevail over granitic rocks. Most of the glass bombs are fresh, especially in the upper portion of the outcrop which represent a chilled zone of the suevite layer. Some 55% of the inclusions in the 4—32 mm size class are glasses. The lower contact of suevite and Bunte Breccia is no longer exposed. The suevite displayed a lower chilled zone at this contact.

References

ABADIAN, M. (1972): Petrographie, Stoßwellenmetamorphose und Entstehung polymikter kristalliner Breccien im Nördlinger Ries. — Contr. Miner. Petrol. **35**, 245—262.

ANGENHEISTER, G. & POHL, J. (1969): Die seismischen Messungen im Ries. — Geol. Bavarica **61**, 304—326.

BIRZER, F. (1969): Molasse und Ries-Schutt im westlichen Teil der Südlichen Frankenalb. — Geol. Bl. NO-Bayern, **19** 1/2, 1—28, Erlangen.

COHEN, A. J. (1961): A semi-quantitative asteroid impact hypothesis of tektite origin. — J. Geophys. Res. **66**, 2521.

— (1963): Asteroid — or comet — impact hypothesis of tektite origin: the moldavite strewn field. — Tektites (ed. by J. A. O'KEEFE), p. 189—211, Chicago Press, Chicago.

CHAO, E. T. C. (1968): Pressure and temperature histories of impact metamorphosed rocks — based on petrographic observations. In: Shock metamorphism of natural materials, B. M. FRENCH & N. M. SHORT (eds.). — Mono Book Corp., Baltimore, 135—158.

DAVID, E. (1969): Das Ries-Ereignis als physikalischer Vorgang. — Geol. Bavarica **61**, 350—378.

DEHM, R. (1969): Geschichte der Riesforschung. — Geol. Bavarica **61**, 25—35.

DENCE, M. R. (1971): Impact melts. — J. Geophys. Res. **76**, 5552—5565.

DENNIS, J. G. (1971): Ries structure, Southern Germany, a review. — J. Geophys. Res. **76**, 5394—5406.

DRESSLER, B., GRAUP, G. & MATZKE, K. (1969): Die Gesteine des kristallinen Grundgebirges im Ries. — Geol. Bavarica **61**, 201—228.

ENGELHARDT, W. v. (1967): Chemical composition of Ries glass bombs. — Geochim. Cosmochim. Acta, **31**, 1677—1689.

— (1974): Die Bildung von Kratern durch den Aufprall extraterrestrischer Massen. — Naturwiss., im Druck.

ENGELHARDT, W. v., HÖRZ, F. (1965): Riesgläser und Moldavite. — Geochim. Cosmochim. Acta **29**, 609–620

ENGELHARDT, W. v., STÖFFLER, D. & SCHNEIDER, W. (1969): Petrologische Untersuchungen im Ries. — Geol. Bavarica **61**, 229—295.

FÖRSTNER, U. (1967): Petrographische Untersuchungen des Suevits aus den Bohrungen Deiningen und Wörnitzostheim im Ries von Nördlingen. — Contr. Mineral. Petrol. **15**, 281—308.

GALL, H. (1974): Geologischer Bau und Landschaftsgeschichte des südöstlichen Vorrieses zwischen Höchstädt a. d. Donau und Donauwörth. — N. Jb. Geol. Paläont. Abh., **145**, 1, 58—95.

GALL, H.; MÜLLER, D. & STÖFFLER, D. (1974): Verteilung, Eigenschaften, und Entstehung der Auswurfmassen des Ries-Impaktkraters. — to be submitted to Geol. Rdsch.

GAULT, D. E. (1973): Displaced mass, depth, diameter, and effects of oblique trajectories for impact craters formed in dense crystalline rocks. — The Moon **6**, 32—44.

GAULT, D. E. & HEITOWIT, E. D. (1963): The participation of energy for hypervelocity impact craters formed in rock. — Proc. 6th Hypervelocity Impact Sympos., Cleveland, Ohio, April 30, May 1—2.

Gault, D. E.; Quaide, W. L. & Overbeck, V. R. (1968): Impact cratering mechanics and structures. — In: Shock metamorphism of natural materials, B. M, French & N. M. Short (eds.). Mono Book Corp., Baltimore, 87—100.

Gentner, W.; Lippolt, H. J. & Schaeffer, O. A. (1963): Argonbestimmungen an Kaliummineralien XI: Die Kalium-Argon-Alter der Gläser des Nördlinger Rieses und der böhmisch-mährischen Tektite. — Geochim. Cosmochim. Acta **27**, 191—200.

Gentner, W. & Wagner, G. A. (1969): Altersbestimmungen an Riesgläsern und Moldaviten. — Geol. Bavarica **61**, 296—303.

Graup, G. (1971): Kristalline Schollen des Nördlinger Ries. — Ph. D. thesis, Tübingen.

Herold, R. (1969): Eine Malmkalk-Trümmermasse in der Oberen Süßwassermolasse Niederbayerns. — Geol. Bavarica **61**, 413—427.

Hörz, F. (1965): Untersuchungen an Riesgläsern. — Beitr. Mineral. Petrogr. **11**, 621—661.

— (1969): Structural and mineralogical evaluation of an experimentally produced impact crater in granite. — Contr. Miner. Petrol. **21**, 365—377.

Hüttner, R. (1969): Bunte Trümmermassen und Suevit. — Geol. Bavarica **61**, 142—200.

Hüttner, R.; Schmidt-Kaler, H. & Treibs, W. (1969): Geologische Übersichtskarte des Ries. — Geol. Bavarica **61**, 451—454 und Beilage.

Johnson, G. G. & Vand, V. (1967): Application of a Fourier data smoothing technique to the meteorite crater Ries. Kessel. — J. Geophys. Res. **72**, 1741—1750.

Jung, K.; Schaaf, H. & Kahle, H. G. (1969): Ergebnisse gravimetrischer Messungen im Ries. — Geol. Bavarica **61**, 337—342.

Kahle, H. G. (1969): Abschätzung der Störungsmasse im Nördlinger Ries. — Z. Geophys. **35**, 317—345.

Kranz, W. (1925—1952): Beiträge zum Nördlinger Ries-Problem. 3.—7. und 9. Fortsetzung: Zbl. Miner. (B) **1925**, 199—201; **1927**, 403—407; **1934**, 262—267; **1937**, 215—216; N. Jb. Miner., Mh. **1945—1948**, 336—339: N. Jb. Geol. Paläont., Mh. **1952**, 49—50.

Löffler, R. (1925): Beiträge zur Riesentstehungshypothese. — Mitt. oberrh. geol. Ver., N.F. **14**, 75—83.

Millman, P. M. & McKinley, D. W. R. (1963): Meteors. — In: B. M. Middlehurst & G. P. Kuiper (eds.), The Moon, Meteorites and Comets, vol. IV of The Solar System, Univ. Chicago Press, 674—773.

Pohl, J. & Angenheister, G. (1969): Anomalien des Erdmagnetfeldes und Magnetisierung der Gesteine im Nördlinger Ries. — Geol. Bavarica **61**, 327—336.

Preuss, E. (1964): Das Ries und die Meteoritentheorie. — Fortschr. Miner. **41**, 271—312.

— (1969): Einführung in die Ries-Forschung. — Geol. Bavarica **61**, 12—24.

— (1971): Über den Bimsstein von Köfels/Tirol. — Fortschr. Miner. **49**, Beih. 1, 70.

Preuss, E. & Schmidt-Kaler, H. (Eds.)(1969): Das Ries. — Geol. Bavarica **61**, 478 p.

Schmidt-Kaler, H. (1969): Versuch einer Profildarstellung für das Rieszentrum vor der Kraterbildung. — Geol. Bavarica **61**, Beilage 5 und S. 38—40.

Schneider, W. (1971): Petrologische Untersuchungen der Bunten Breccie im Nördlinger Ries. — N. Jb. Miner. Abh. **114**, 136—180.

Shoemaker, E. M. & Chao, E. T. C. (1961): New evidence for the impact origin of the Ries basin, Bavaria, Germany. — J. Res. Geophys. **66**, 3371—3378.

Staehle, V. (1970): Nickel und Kobalt in Gesteinen des Nördlinger Ries. — Contr. Miner. Petrol. **28**, 72—88.

Stöffler, D. (1965): Anzeichen besonderer mechanischer Beanspruchung an Mineralien der Kristalleinschlüsse des Suevits (Stoßwellenmetamorphose). — N. Jb. Miner. Mh. **1965**, 9—11, 350—354.

— (1966): Zones of impact metamorphism in the crystalline rocks of the Nördlinger Ries crater. — Contr. Miner. Petrol. **12**, 15—24.

— (1971b): Coesite and Stishovite: identification and formation conditions in shock metamorphosed rocks. — J. Geophys. Res. **76**, 5474—5488.
— (1971a): Progressive metamorphism and classification of shocked and brecciated crystalline rocks at impact craters. — J. Geophys. Res. **76**, 5541—5551.
— (1972): Deformation and transformation of rock-forming minerals by natural and experimental shock processes. I. Behavior of minerals under shock compression. — Fortschr. Miner. **49**, 50—113.
— (1974): Deformation and transformation of rock-forming minerals by natural and experimental shock processes, II. Physical properties of shocked minerals. — Fortschr. Miner. **51**, 256—289.
Stöffler, D.; Gall, H. & Müller, D. (1974): Distribution and properties of the ejecta deposits at the Ries impact structure. — in prep.
Storzer, D.; Horn, P. & Kleinmann, B. (1971): The age and the origin of the fused rock from the Köfels structure, Austria (Abstract). — Meteoritics **6**, 319—320.
Stutzer, O. (1936): Meteor Krater und Nördlinger Ries. — Z. Deut. Geol. Ges. **88**, 510—523.
Waters, A. & Fisher, R. V. (1971): Base surges and their deposits: Capelinhos and Taal volcanoes. — J. Geophys. Res. **76**, 5596—5614.
Werner, E. (1904): Das Ries in der schwäbisch-fränkischen Alb. — Bl. schwäb. Albverein **16**, 153—167.
N. N. (1974): Die Forschungsbohrung Nördlingen 1973. — Geol. Bavarica **72**, München.